Riera-Guasp, M.; J. Antonino-Daviu; Rusek, J.; José Roger-Folch (2009). Diagnosis of rotor asymmetries in induction motors based on the transient extraction of fault components using filtering techniques. Electric Power Systems Research. 79(8):1181-1191. doi:10.1016/j.epsr.2009.02.009

Diagnosis of rotor asymmetries in induction motors based on the transient extraction of fault components using filtering techniques

M. Riera-Guasp* J. Antonino-Daviu* J. Rusek** J. Roger-Folch*

* Universidad Politécnica de Valencia
Departamento de Ingeniería Eléctrica
P.O.Box 22012, 46071 Valencia, SPAIN
Phone: 0034-96-3877592, Fax: 0034-96-3877599
e-mail: joanda@die.upv.es

** Dept. Electrical Engineering
AGH University of Science and Technology
Al. Mickiewicza 3, 030-059 Krakow, POLAND
Phone: 0048-12-6172823, Fax: 0048-12-6341096
e-mail: gerusek@cyf-kr.edu.pl

Abstract: The aim of this paper is to present and validate a methodology for diagnosing rotor asymmetries in cage motors, based on the analysis of the stator startup current. The method consists of the extraction of a harmonic component introduced by this fault- *the left sideband component*- from the stator startup current. Two alternative techniques developed by different research groups are proposed for the transient extraction of this component; the Digital Low Pass Filtering (DLPF) and the Discrete Wavelet Transform (DWT). Both approaches are applied to three different industrial motors ranging from 1.1 to 450 kW. A detailed explanation of the physical basis of the method and comments related to the application scope of the approach are also given. The results show the robustness of both approaches for the reliable diagnosis of the fault, and suggest a clear potentiality for extending the methodology to the detection of other types of faults introducing components dependant on the slip.

1. INTRODUCTION

The diagnosis of rotor faults in induction motors is a problem with unquestionable industrial interest in the field of the predictive maintenance of electrical machines; this type of failure amounts for a significant percentage on the faults feasible to occur in this type of machines [1]. In addition, the costs that it might cause, if it is not diagnosed in time, can be huge.

The diagnosis of rotor asymmetries in asynchronous machines has been deeply studied by many authors; a review of the bibliography on this field can be found in [2]. Basically, the different diagnosis methods proposed can be classified following two different criteria:

- *According to the physical quantity analysed for monitoring the rotor condition*; diagnosis methods based on the measurement of vibrations [3], fluxes on search coils [4], axial flux on coils concentric with the shaft [5], air-gap torque [6], instantaneous power [7], residual voltages during the disconnection [8] or stator currents [1, 9-11] have been proposed; the methods based on the measurement of the stator current have drawn most of the attention in the industrial environment, since this signal can be obtained directly from the already existing current transformers, avoiding the installation of any specific probe or any interruption on the operation of the machine.

- *According to the operation regime of the machine when the measurement is done*. There are two possibilities: monitoring magnitudes in steady-state or during transient operation. Initially, diagnosis methods based on steady-state analysis were developed; they have become the most used in the industrial environment. However, during these last years, thanks to the advances done in the signal processing field, diagnosis techniques based on the transient analysis have been introduced. These methods have proven their validity for some applications [12-18].

However, despite the multiple existing references, the detection of rotor faults cannot be considered a problem completely solved. The difficulty of the diagnosis is due to the inherent characteristics of this fault:

Firstly, due to the constructive characteristics of the squirrel-cage rotor, the direct measurement of electrical magnitudes in this part of the machine is not possible.

Moreover, during the real operation of the motors, a bar breakage does not produce apparent symptoms; no significant increases in the temperature, demanded currents or slip appear; furthermore, no substantial increment neither in the noise nor even in the vibrations is produced.

Nevertheless, if the fault is not diagnosed during its early stages, it gets worse, propagating towards the adjacent bars, appearing local hot spots and interbar currents that can damage the magnetic circuit [19]. If this stage of the fault is reached, some symptoms enabling its easy diagnosis appear; however, the repair has a much higher cost or it may even be unfeasible. Therefore, an efficient diagnosis method should be sensitive enough for detecting the fault in its incipient state.

Another feature that every system for the detection of rotor faults should achieve is the reliability of its diagnostics; this means that the probability of occurrence of a wrong positive diagnostic, induced by causes different from a rotor failure, should be very low. This characteristic is crucial, mainly when diagnosing large machines, in which the interruption, disassembly, and reassembly costs can be very important.

It has to be remarked that none of the diagnosis methods hitherto introduced is capable to guarantee the sensitivity and reliability required in the industrial environment for all the possible utilization conditions of the induction motors. Indeed, when facing a specific problem, the first step for reaching a diagnostic should be the selection of the most suitable method for the utilization conditions of the machine.

In this paper, two alternative approaches for rotor fault diagnosis based on the analysis of transient stator currents are ~~presented~~ applied to different machines under real operation conditions. It is shown that both methods, developed by two different research groups, share the same physical basis: the extraction during the startup transient of the left sideband component caused by the breakage, from the stator current signal. Nevertheless, these methods employ different signal processing tools for this purpose. The first approach

is based on the use of a digital low-pass filter which extracts the evolution of the sideband component under a predefined cut-off frequency. The second method is based on the application of the Discrete Wavelet Transform (DWT) to the startup current signal and the subsequent study of the approximation signal covering the range of frequencies through which the left sideband evolves [14, 20-21]. Both methods are applied to different industrial machines (ranging from 1.1 to 450 kW and with different number of poles) under various load conditions. Results show the validity of both techniques for the diagnosis of rotor asymmetries, especially when the startup length is not too short. In this situation, the methods are proven to be enough sensitive to detect even a single bar breakage, enabling a very reliable diagnostic.

Another goal of this paper is to extend the validation of the approach developed in [20] to machines with large sizes, supplied with high voltage and with double cage, working under real industrial conditions, as well as to show the flexibility of the DWT approach for bringing a reliable diagnostic, even when non related fault components distort the characteristic pattern of the fault.

The paper is organized as follows: Section 2 reviews the physical bases of the rotor fault diagnosis methods based on stator current analysis; the scope of application of steady-state and transient based methods is commented. In Section 3, the diagnosis technique based on low pass filtering (DLPF) is presented and validated by tests. Section 4 deals with the method based on the DWT analysis, which is also introduced and validated. Finally, the conclusions of the work are presented.

2. PHYSICAL FOUNDATIONS OF THE METHOD

The diagnosis of cage asymmetries can be based on the examination of different signals of electrical, magnetic or mechanical nature. Nevertheless, as it was commented before, in the industrial environment, the supply currents are the most used signals for diagnosis purposes.

2.1. Diagnosis based on the analysis of the steady-state stator current.

The physical bases for most of the diagnosis approaches based on stator current analysis were introduced by Kliman, Elkasabgy, Thomson and others [22-23]: when a rotor bar breaks, the current cannot circulate through it and, consequently, a perturbation (or fault field) in the magnetic air-gap field appears. In steady state, the fault field induces some current components in the stator windings, with characteristic frequencies. Depending on the constructive parameters of machine and the total inertia of the group, these frequencies can be calculated by (1) and (2):

$$f_b = (1 \pm 2 \cdot k \cdot s) \cdot f \qquad k = 1,2,3.... \tag{1}$$

$$f_b = \left(\frac{k}{p}(1-s) \pm s \right) \cdot f \qquad \frac{k}{p} = 1,3,5.... \tag{2}$$

where f_b: detectable bar breakage frequencies; p: number of pole pairs; f : supply frequency; s: slip.

Among these current components, the most relevant is that known as *left sideband harmonic* (f_{Ls}), with frequency given by (3):

$$f_b = (1 - 2 \cdot s) \cdot f \tag{3}$$

The diagnosis principle of the approaches based on the harmonic analysis of the steady-state stator current basically consists of finding some of these components (mainly the left sideband component) within the spectrum of the sampled current signal.

Regarding the sensitivity and reliability of these approaches, the following facts should be remarked:

- The amplitudes of the fault components in the stator current are load-dependant. In a machine with a single bar breakage working under full load, the sideband components can reach roughly one per cent of the amplitude of the fundamental component [14]. This amplitude decreases when the load does, so the sensitivity of the diagnosis becomes very poor in machines working with light loads.

- The frequencies of the fault components depend on the slip; when the slip decreases, these

frequencies get closer to the values for the frequencies of the usual harmonics present in healthy machines (the fundamental or higher order harmonics produced by windings distribution or saturation); so the reliability of the diagnosis also decreases when the load reduces.

- The resolution reached in the determination of the harmonic frequencies of a sampled signal depends on the length of the sampling interval. A high resolution implies a long sampling interval, and this is only possible if the machine works strictly in steady state. Load or voltage fluctuations cause uncertainty in the frequencies of the fault components [11, 14]; subsequently, the fault harmonics can be confused with harmonics with similar frequencies caused by other phenomena. This means that the reliability of the diagnosis also reduces when the uniformity of the machine regime decreases.

Therefore, in general, the steady-state analysis approaches are suitable for applications in which the machine works near the full load condition and under a strict steady-state regime.

2.2. Diagnosis based on the analysis of the stator startup current.

In order to avoid these disadvantages, recent methods based on the detection of the left sideband component during the startup transient have been proposed. The diagnostic techniques based on the transient analysis applied to critical machines are usually integrated within predictive maintenance programs, in which the machines are continuously monitored. The application of these techniques does not imply any disturbance in the operation of the machines, since the measurements of the transient currents are carried out taking advantage of the startups of the normal working cycle of the motor.

For not too fast startups, once the electromagnetic transient is finished, it can be assumed that the machine accelerates following a succession of stationary regimes, with increasing speeds. Under these conditions, the left sideband harmonic has a continuous evolution, changing its frequency with the slip, as indicated by (3). This frequency evolves in a particular way; it starts being equal to 50 Hz, at the time when the machine is connected (s=1). As the rotor accelerates, the frequency drops, reaching 0 Hz when

the slip equals to 0.5. From this time, it increases again reaching nearly 50 Hz, when the steady-state regime is reached (s≈0). Figure 1 shows the calculated evolution of left sideband for a startup of a 1.1 kW squirrel cage machine with a broken bar. This evolution was justified theoretically by the authors in [20]. The reader can see Appendix I for further information.

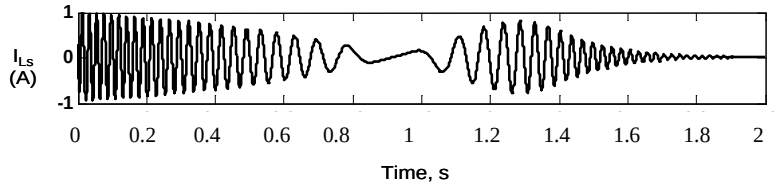

Figure 1. Evolution of the left sideband component in amplitude and frequency during the startup transient.

Some methods based on this phenomenon have been proposed during these last few years for detecting this component, using different signal analysis techniques. In this sense, Watson and others [12, 13] propose the detection of the component through the convolution of the current signal with a Gaussian wavelet. In [15], the DWT coefficients are used for the diagnosis. The method proposed in [16] is based on the use of the wavelet ridge. [14, 21] describe a characteristic pattern in the low-frequency wavelet signals, resulting from the DWT of the startup current, as an evidence of the evolution of the left sideband component during this transient.

It has to be remarked that when using approaches based on the transient analysis, the load condition of the induction motor is not important; despite this, these methods need a minimum inertia factor of the group leading to startup times longer than around 0.5 seconds. This is necessary in order to avoid the influence of the initial electromagnetic transient, taking place after the connection of every machine, and the border effects, which in the earlier stage of the startup transient mask completely the sideband component. On the other hand, the larger the length of startup process, the clearer the left sideband evolution is and, so, the better the reliability of the diagnosis. Thus, the approaches based on transient

analysis are especially suitable for applications with heavy startup transients (high inertia factors, long startup lengths). Indeed, these are the cases in which a bar breakage is more likely to occur.

In any case, the limitations and application scope of the transient and steady-state approaches are clearly different. The crux of the matter is not if one is better than the other, but which is more suitable for a specific application.

This paper proposes and compares two methods for the diagnosis of rotor bar breakages, based on the extraction of the left sideband harmonic from the startup current; the first technique uses a digital low pass filter, whereas the second is based on the application of the Discrete Wavelet Transform (DWT) for this purpose. Both methods enable the direct extraction of the evolution of the left sideband harmonic during the startup process. They are quite different from the transient-based approaches commented above, where this component was detected in an indirect way, by means of the alterations that it causes on different parameters or signals associated with the startup process. Therefore, both of them enable a clear interpretation of the physical phenomenon taking place in the machine, relating the oscillations occurring in the diagnosis signals with the physical evolution of the fault component during the transient.

Another important advantage of the proposed methods is the very high reliability of the diagnosis, since it is very unlikely that the characteristic waveform of left sideband during the startup may be caused by other phenomena different from a rotor fault.

Moreover, the introduction of non-dimensional parameters for the quantification of the degree of severity of the fault complements the qualitative detection of the characteristic patterns caused by the left sideband evolution, ~~strengths the reliability of the proposed approaches.~~ These parameters are useful for the automatic detection of the faults in monitoring systems, since it is easier to detect when the fault parameter exceeds a previously preset threshold value than recognizing a pattern within a signal. When the fault parameter exceeds the threshold value, the system would generate an alert and an off-line analysis of the current could be carried out, in order to reach a reliable diagnostic.

3. DIAGNOSIS BASED ON THE LEFT SIDEBAND EXTRACTION USING LOW-PASS FILTERING.

Authors of this paper took part in the elaboration of a diagnostic system based on the low pass filtering of the startup current signal [24]. The system relies on one digitally registered supply current. The registration can be achieved with any equipment, containing an analog-to-digital converter. The results presented next are based on the currents flowing in the secondary winding of current transformers, accessed via current clips. The current clips voltage signal is delivered to a portable computer fitted with an analog-to-digital converting card. The registered startup currents are stored on the disc and are then analyzed offline by the low-pass-filtering based diagnostic system. The system accounts for the correction characteristic resulting from frequency transfer functions of the current transformer, passive current clips, low pass and antialiasing filter. The cut-off frequency assumed for the low pass filtering is 25 Hz.

The application of this technique enables obtaining a diagnosis signal I_{LP}, which contains the time evolution of the components of the original startup current signal with frequencies below the predefined cut-off frequency (25 Hz). Table I resumes the main characteristics of the low pass filter used. It can be synthesized using the "Filter Design & Analysis Tool" (fdatool) of MATLAB.

Table I
Filter characteristics

Filter Type	Low pass
Design method	FIR (least-squares)
Order	2000
Sampling frequency (F_s)	4096 Hz
End of the passband (F_{pass})	25 Hz
Begining of the stopband (F_{stop})	30 Hz
Passband weigthing (W_{pass})	1
Stopband weigthing (W_{stop})	100

Figure 2 shows the application of the low-pass filtering technique for the case of a 200 kW machine with rotor asymmetry; the upper graph is the startup current signal, the graph in the middle corresponds to the diagnosis signal I_{LP}, whereas the graph below is a zoom of the central region of this diagnosis signal

I_{LP}. It is observed a particular waveform for I_{LP}, showing clear similarities with the theoretical waveform for the left sideband component during the transient, shown in Figure 1. Thus, the amplitude of this signal is in direct relation with the level of presence of the sideband component in the machine and, consequently, with the level of asymmetry. Otherwise, if the machine is healthy, the amplitude of the signal would remain very low, since the sideband component will not be present (or it will have a very low value due to the own imperfections of the rotor). Therefore, this signal becomes a reliable indicator of the presence of the fault.

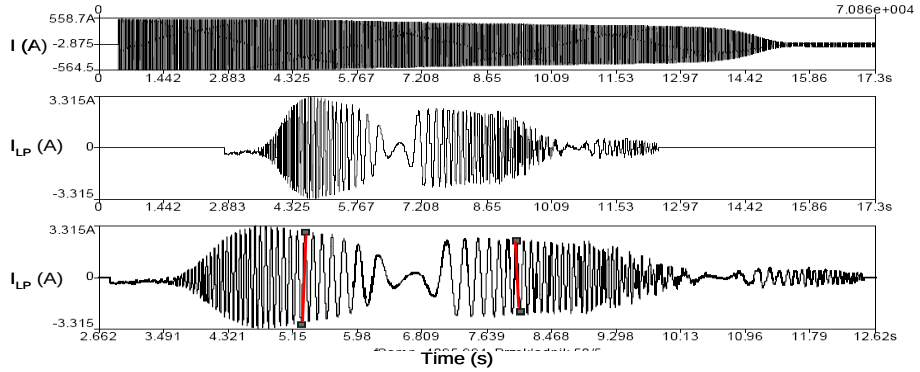

Figure 2. Application of the low pass filtering technique to the startup current for a 200 kW machine with rotor asymmetry.

Considering all these facts, a quantification indicator based on the amplitude of this diagnosis signal was developed by the authors. This indicator is defined as follows:

- Firstly, the amplitude of the signal I_{LP} is computed when its frequency reaches a value of 10 Hz, during the interval in which the frequency decreases from the supply frequency to zero (see Figure 2).
- Second, the amplitude of the signal I_{LP} is again computed but when its frequency is equal to 10 Hz, during the interval in which the frequency increases again up to the supply frequency (see Figure 2).
- The ratios between each one of the amplitudes and the amplitude of the startup current signal at the time when the frequency of 10 Hz occurs are computed.
- The diagnosis indicator γ_{LP} is defined as the average of both ratios.

Consequently, the indicator γ_{LP} is defined as dependant on the amplitude of the diagnosis signal at a particular frequency (10 Hz). The selection of that particular frequency is justified by the previous experience, reached after the vast amount of industrial diagnoses done with this technique; for this particular frequency, the influence of the oscillations introduced by the electromagnetic transient is reduced, since when this frequency occurs, these oscillations have already attenuated. According to the experience, a threshold value for γ_{LP} equal to 0.8% is considered to mean that a significant level of asymmetry exists in the machine (at least one broken rotor bar).

3.1. Case I: Laboratory tests on a 1.1 kW induction motor with a broken bar.

Figures 3 and 4 illustrate the application of the low pass filtering technique to startup signals obtained from laboratory tests carried out on an industrial cage motor rated 1.1 kW, 400 V, star-configuration, 4 poles and 28 rotor bars. The motor was started direct on line, driving a load with a negligible resistant torque and an inertia factor IF=10, leading to a startup length of 1.6 seconds.

The machine was tested firstly in healthy condition (Figure 3) and then, after forcing a rotor bar breakage (Figure 4). Figure 5 shows the tested motor and its rotor with a bar breakage.

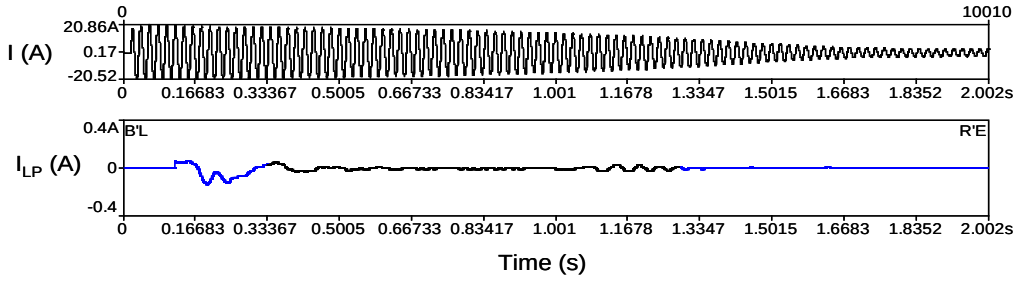

Figure 3. Low pass filtering diagnostic of the 1.1 kW motor (healthy condition).

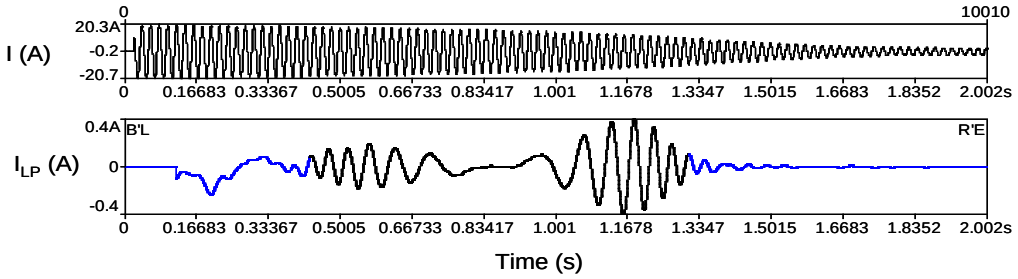

Figure 4. Low pass filtering diagnostic of the 1.1 kW motor (1 broken bar)

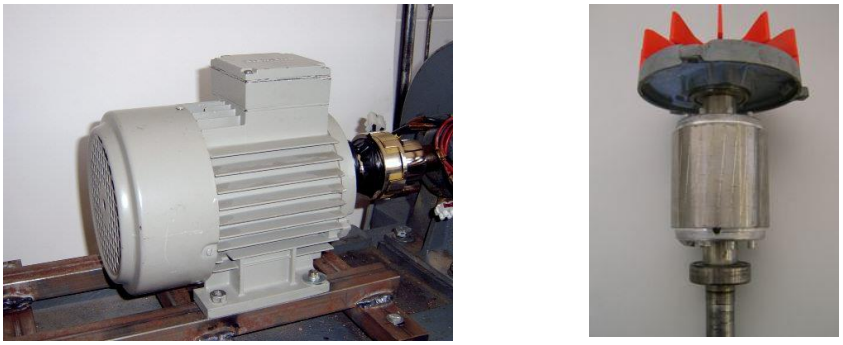

(a) (b)

Figure 5. (a) Tested motor. (b) Rotor with a bar breakage

In Figures 3 and 4, the graphic on the top is the sampled startup current (I), whereas the graphics below show the diagnosis signal (I_{LP}). There are clear differences between these waveforms. For the healthy machine the signal I_{LP} remains practically null, whereas in the case of faulty machine (Figure 4), this signal is very similar to the theoretical waveform for the left sideband component shown in Figure 1, within the time interval $0.45<t<1$. Therefore, it can be concluded that for the machine with a broken bar, the low-pass filtering enables the extraction of the left sideband component for the frequencies below the cut-off frequency of the filter (25 Hz).

The diagnosis indicator γ_{LP} for the healthy machine (Figure 3) amounted for a very low value (0.11%), confirming the healthy condition of the motor. On the other hand, the value for γ_{LP} in the

case of the machine with 1 broken bar (Figure 4) was equal to 1.8%, a value confirming the presence of the significant asymmetry in the motor for that case.

3.2. Case II: 850/450 kW healthy motor driving a fume exhausting fan.

The machine under diagnosis was a 850/450 kW double speed motor operating at 450 kW (lower speed, number of pole pairs= 5). It was driving a fume exhausting fan in a Power Generation plant. The application of the low-pass filtering technique is shown in Figure 6. A very low level of asymmetry is detected, as reflected by the low amplitude of in the diagnosis signal I_{LP}. This is confirmed by the low value of the parameter used for the quantification of the severity of the fault (γ_{LP}=0.076 %). Therefore, the asymmetry may be caused by the own defects of the rotor due to the manufacturing process. These results can be taken as a reference of healthy machine when machines with similar characteristics are diagnosed.

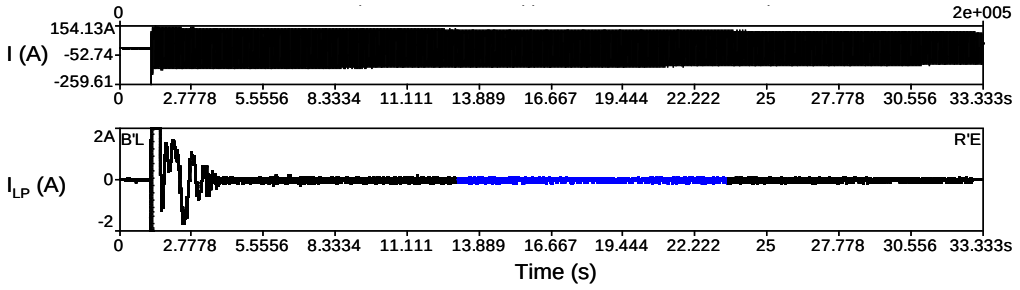

Figure 6. Low pass filtering diagnostic of the 850/450 kW machine in Case II.

3.3. Case III: 850/450 kW induction motor, with possible asymmetry, driving a smoke fan.

Figure 7 corresponds to a two speed squirrel cage induction machine with a number of pole pairs p = 4 or 5; the machine drives a smoke fan in a Power Generation plant. This machine is very similar to that diagnosed in the previous section. The upper graph shows the startup current corresponding to p = 5, this is, for the lower speed. The startup is accomplished within about 30 seconds. The signal below is the diagnosis signal I_{LP}.

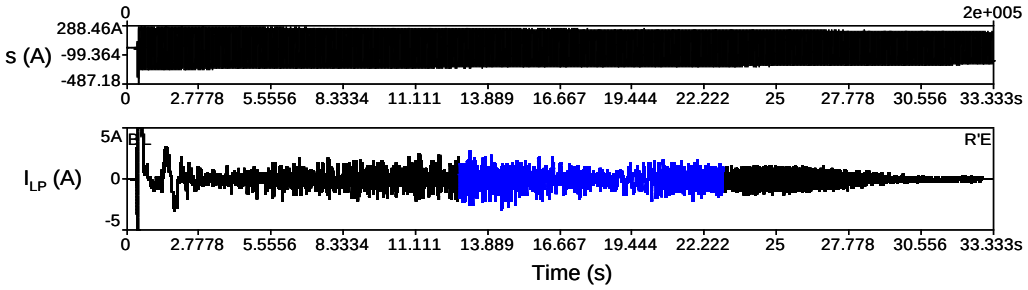

Figure 7. Low pass filtering diagnostic of the 850/450 kW machine in Case III.

The higher amplitude of the diagnosis signal if compared with that of the previous case is clearly observed. The reason is the higher level of asymmetry present in this machine, which is confirmed by the value for the quantification indicator γ_{LP}=0.95%, more than ten times that obtained for the previous case. However, the evolution of the diagnostic signal does not fit clearly the characteristic shape of the sideband component during the startup; so, this case is diagnosed as a possible fault, and further tests would be necessary to confirm the diagnostic

3.4. Case IV: 400 kW induction motor with clear asymmetry driving a coal mill fan

Figure 8 corresponds to a 400 kW squirrel cage induction machine driving a coal mill fan and operating under real conditions in a Power Generation plant. The number of pole pairs is p = 2.

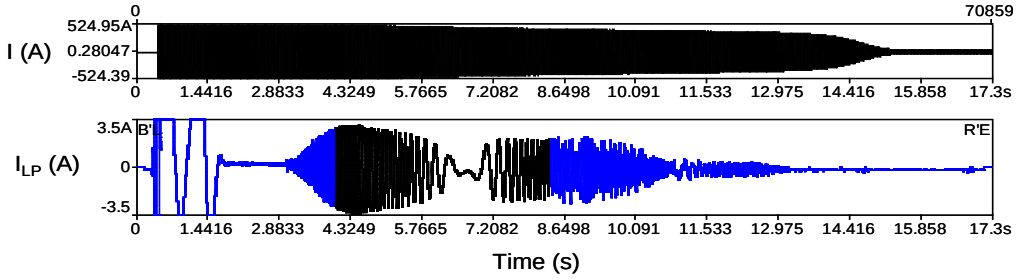

Figure 8. Low pass filtering diagnostic of the 400 kW machine.

The signal in Figure 8 reveals a waveform for the diagnosis signal I_{LP} fitting quite well the central region of the theoretical evolution of the left sideband component, shown in Figure 1. This is because this signal, as commented before, is reflecting the time evolution of the components with frequencies below the predefined cut-off frequency (25 Hz). Therefore, this signal constitutes a partial representation of the left sideband evolution; it shows the evolution of this component within the frequency range [0-25] Hz. For the signal in Figure 8, the diagnostic indicator γ_{LP} amounts for 0.81%. This value confirms that a certain level of asymmetry exists in the machine, although on the threshold for being considered as significant.

4. DIAGNOSIS BASED ON THE LEFT SIDEBAND EXTRACTION USING THE DISCRETE WAVELET TRANSFORM

This section explains the main concepts and practical details in order to understand the application of the Discrete Wavelet Transform for extracting the left sideband component from the startup current. Further details on Wavelet theory can be found in the specialized literature [25-26].

The Discrete Wavelet Transform performs the decomposition of a sampled signal ***s(t)*** (s_1, s_2, …s_N) onto n+1 wavelet signals: an approximation signal a_n(t) and n detail signals d_j (t) with j varying from 1 to n:

$$s(t) = a_n + d_n + \ldots + d_1 \tag{4}$$

The parameter n is an integer known as "number of decomposition levels". In order to extract the left sideband, n must be set to a specific value which will be justified below, which is a function of the sampling rate f_s of ***s(t)*** .

Conceptually, the *detail signal* d_1 is calculated as:

$$d_1(t) = \sum_i \beta_i^1 \cdot \boldsymbol{\psi_i^1(t)} \tag{5}$$

Where β_i^1 are the wavelet coefficients (real numbers), ψ_1^1 is the mother wavelet (the base function used for the decomposition); the functions ψ_i^1 are identical to the mother wavelet but shifted in time by $\Delta t = i/T$, being T the sampling period of ***s(t)***.

The *detail signal* d_j is calculated in a similar way, but using as a base the wavelet with level j, which is a scaled and time expanded version of the mother wavelet

$$dj(t) = \sum_i \beta_i^j \cdot \boldsymbol{\psi_i^j(t)} \tag{6}$$

The *approximation signal* a_n is obtained similarly, but using the known as scaling function φ_j^n and scaling coefficients α_j^n, instead of the wavelet function and coefficients:

$$a_n = \sum_i \alpha_i^n \cdot \boldsymbol{\varphi_j^n(t)} \tag{7}$$

Each mother wavelet is associated with a family of scaling functions, which are perfectly determined once the mother wavelet is selected.

The most relevant concept regarding the extraction of the left sideband is that the DWT behaves as a bank of digital filters; each one of the n+1 signals resulting from the transform approximately represents the time evolution of the components of the original signal belonging to a specific frequency band.

Figure 9 is a qualitative representation of the transfer functions of the filters used in the transform. The resulting frequency bands are consecutive; the limits for these bands depend on the level of the signal and on the sampling rate. For the detail d_1, the upper limit is half the sampling rate ($f_s/2$), whereas the lower limit is $f_s/4$. For a generic detail d_n, the upper limit of its frequency band coincides with the lower limit of the band of the previous detail d_{n-1}, and its bandwidth is half the bandwidth of the previous detail.

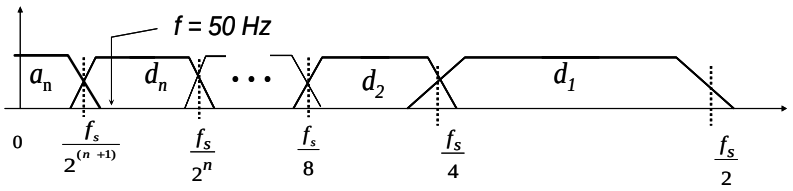

Figure 9. Frequency bands corresponding to the DWT signals

Therefore, a generic detail d_n contains the information concerning the signal components with frequencies included within the interval $[2^{-(n+1)} \cdot f_s , 2^{-n} \cdot f_s]$ Hz. On the other hand, the approximation a_n contains the low frequency components of the original signal included in the interval $[0, 2^{-(n+1)} \cdot f_s]$ Hz.

Moreover, Figure 9 shows that the DWT does not perform an ideal filtering process; a certain overlap between adjacent bands always exists [27].

If the number of decomposition levels n is selected so that the detail d_n contains the frequency of the supply source (f), then the approximation with the same level, a_n, only contains signal components with frequencies below f, as it can be observed in Figure 9.

If the DWT is applied to the startup current of a healthy machine, these low frequency components are negligible, once the low frequency oscillations caused by electromagnetic connection transient are extinguished. When this transient is finished, a_n remains practically null.

Otherwise, if a bar breakage exists, the left sideband harmonic has a significant amplitude throughout the startup transient; since its frequency is always below 50 Hz, this component is contained within the approximation signal a_n during almost the whole startup process; since no other significant component exists within this signal, the characteristic waveform of the left sideband can be clearly recognized in the approximation a_n. This enables a very reliable diagnosis of bar breakages, as it is proved in the cases analysed below.

Regarding the practical details for the application of this approach, the DWT was carried out using the standard Matlab Wavelet Toolbox software. For this purpose, three parameters must be selected:

- *Type of mother Wavelet*: several wavelet families (Daubechies, Simlet, Biorthogonal, dmeyer, Gaussian…), have behaved satisfactorily for the extraction of the left sideband [21], despite their different mathematical properties.

- *Order of mother wavelet*: This parameter influences the ideal characteristic of the filtering process [21, 27]. High order mother wavelets reduce the overlap between adjacent frequency bands and, therefore, they enable a clearer identification of the sideband component evolution. This is due to the better frequency response of the associated filter.

- *Number of levels of decomposition (n)*: in order to contain the left sideband evolution within the approximation a_n, the upper limit of its associated frequency band has to be set below the supply frequency *f*; since this limit depends on the sampling rate, this condition implies [21]:

$$n = Integer\left[\frac{\log(f_s / f)}{\log(2)}\right] \tag{8}$$

In the next part of this Section, the method for the extraction of the left sideband based on the DWT is applied to the same four cases presented in Section 3; DWT analysis is carried out using the same startup current signals used for the low pass filtering technique. Daubechies-44 is used as mother wavelet, due to its good frequency response and, as explained above, more ideal filtering characteristic. In each case, the sampling frequency used for capturing the signals is specified, as well as the frequency range covered by the approximation signal used for the diagnosis.

4.1. Case I: Laboratory tests on a 1.1 kW induction motor with a broken bar.

Figures 10 and 11 illustrate the application of the DWT method to the industrial cage motor rated 1.1 kW. The sampling frequency used for capturing these signals was f_s= 5000 samples/s. Thus, according to (8) the number of decomposition levels has to be set to n=6. The frequency band covered by the approximation signal a_6 is [0-39] Hz. Figure 10 corresponds to the analysis under healthy unloaded condition, whereas Figure 11 shows the analysis of the startup current for the unloaded motor with one broken bar.

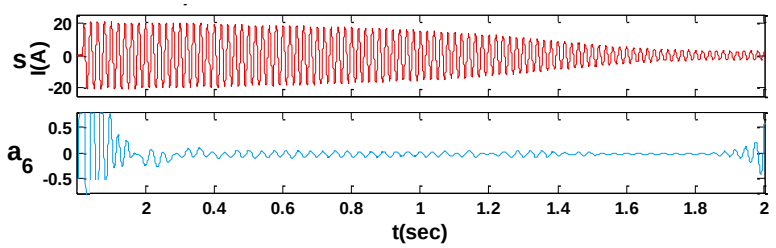

Figure 10. DWT of the 1.1 kW machine under healthy unloaded condition.

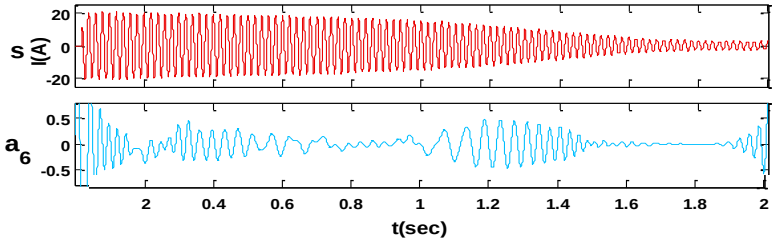

Figure 11. DWT of the 1.1 kW unloaded machine with one broken bar.

The upper graphs of the figures correspond to the sampled stator startup currents, whereas the lower graphs are the approximation signals a_6 obtained after applying the DWT to the current. Comparing both figures, clear differences can be observed between the evolution of the approximation signal a_6 for the healthy and faulty cases. Indeed, for the machine with one broken bar, the approximation a_6 shows a frequency evolution (first decreasing, becoming zero, and then increasing) fitting that of the left sideband. Moreover, its evolution in amplitude is also quite characteristic, fitting approximately the theoretical evolution of the left sideband shown in Figure 1.

The reason for the slight differences between the waveform for the approximation signal a_6 and that for the left sideband, shown in Figure 1, is that the upper limit of the approximation signal is not exactly 50 Hz, but 39 Hz. The reason for setting an upper limit for the approximation signal slightly lower than the supply frequency is to avoid the partial filtering of the supply frequency component within that signal, due to the fact that a certain non ideal characteristic of the filter is always present, despite the selection of a high order mother wavelet.

Therefore, this approach enables a reliable diagnosis of the rotor fault, even in the case of a machine with a single bar breakage.

A non-dimensional parameter, based on the energy of the approximation signal used for the diagnosis, can be proposed for the quantification of the degree of severity of the fault. This parameter γ_{AP} is defined as the ratio between the energy of the approximation signal and the energy of the stator startup current signal, according to the following expression:

$$\gamma_{AP}(dB) = 10 \cdot \log\left[\frac{\sum_{j=Nb}^{Ns} i_j^2}{\sum_{j=Nb}^{Ns}[a_n(j)]^2}\right] \tag{9}$$

where i_j is the value of the j sample of the current signal; a_n (j) is the j element of the order n approximation signal; N_s is the number of samples of the signal, until reaching the steady-state regime and N_b is the number of samples between the origin of the signals and the extinction of the oscillations due to border effect.

The value for the parameter γ_{AP} computed for the 1.1 kW motor under healthy condition (Figure 10) amounts for 46 dB, whereas its value for the machine with one broken bar (Figure 11) is equal to 35.1 dB. The much lower value for the second case confirms the existence of a fault in the machine.

4.2. Case II: 850/450 kW healthy motor driving a fume exhausting fan.

Figure 12 shows the application of the DWT method to the startup current signal for this case. In this csase, the sampling frequency used for capturing the signal was f_s= 6000 samples/s. Thus, according to (8) the number of decomposition levels has to be set to n=6. The frequency band covered by the approximation signal a_6 is [0-46.9] Hz. Due to the proximity between the upper limit of the approximation signal and the supply frequency, a number of levels n=7 has been considered, in order to avoid the partial filtering of the supply frequency component in the band covered by the approximation [14]. Hence, in this case, the range of frequencies covered by a_7 is [0-23.5] Hz.

The amplitude of the approximation signal used for the diagnosis is very low. This informs about the healthy condition of the machine; only some very slight oscillations appear, according to the characteristic pattern associated with the anomaly. They can be due to the imperfections of the rotor cage commented above. The value for the quantification parameter γ_{AP} is this case is 107.5 dB.

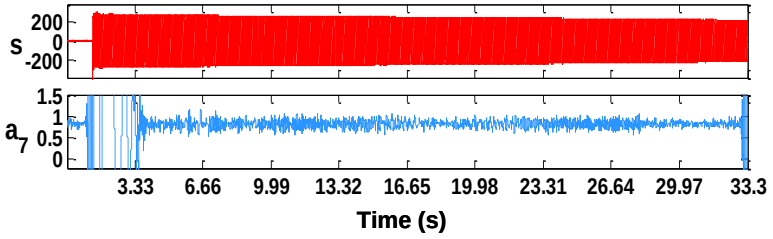

Figure 12. Tested current and approximation a_7 for the startup of the machine of the Case II.

4.3. Case III: 850/450 kW induction motor, with possible asymmetry, driving a smoke fan

Figure 13 shows the startup current signal (upper graph), the approximation signal used for the diagnosis (graph in the middle) and a zoom of the central region of this signal (graph below). The same comments regarding the sampling frequency and the selection of the approximation signal, made for the previous case, are valid here.

The approximation a_7 in that figure clearly shows the characteristic frequency evolution of the sideband component during the increasing zone (18.3 < t < 21.6). However, the decreasing and null zones are not so clear. Thus, the diagnostic of rotor fault in this case is less evident than in the previous ones. In any case, as it is shown below, in this situation, the characteristic evolution of the sideband component is partially masked by another harmonic component with frequency below 50 Hz, caused by another phenomenon not related with the bar breakage.

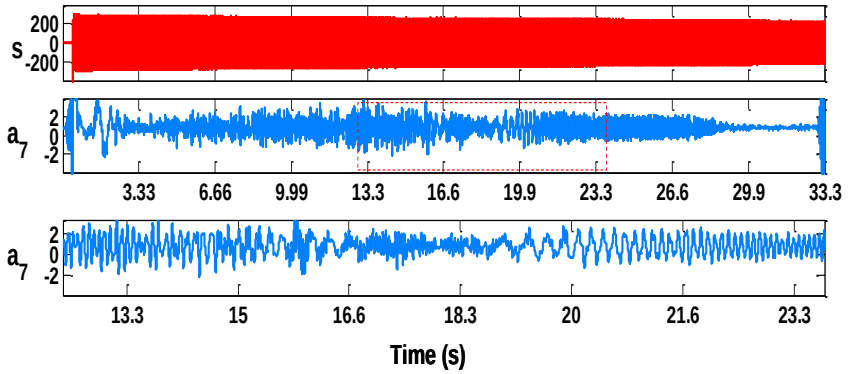

Figure 13. Tested current, approximation a_7, and a zoom of a_7 for the startup of the machine of Case III.

In order to increase the reliability of diagnosis, a complementary method for detecting the sideband component by means of the DWT can be applied, such as the one proposed in [14]. Figure 14 shows the result of the application of this method to the machine under study. The method, also based on the application of DWT to the startup current, consist of analyzing the wavelet signals with level higher than *n* (signals with frequency bands below the supply frequency). In [14] it is proved that, in the case of bar breakages, a characteristic pattern appears on these signals; the fault creates oscillations within the wavelet signals, arranged in such a way that they reflect the frequency evolution of the sideband component through the startup transient; this pattern is clearely shown in Figure 14. Thus, a reliable diagnostic of the asymmetry is achieved with this analysis. The quantification parameter γ_{AP} computed in this case, amounts for 99.8 dB, a value lower than in the previous case, which confirms the higher level of asymmetry in this machine.

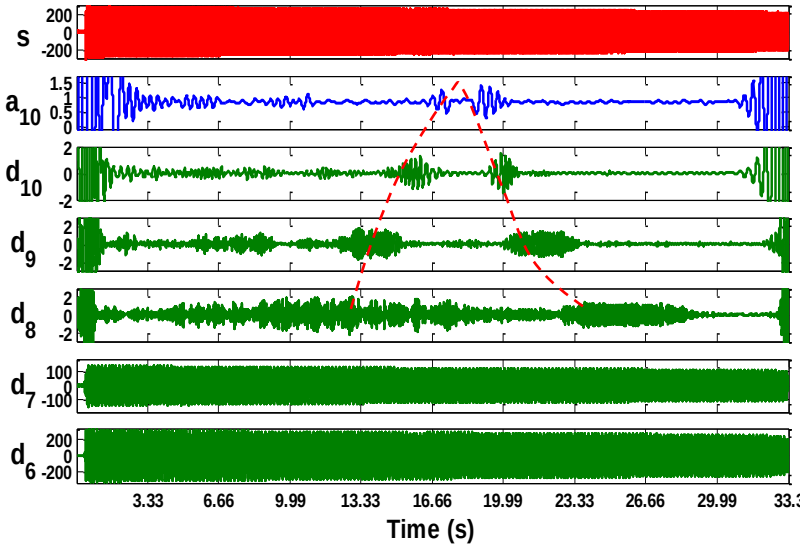

Figure 14. Alternative DWT analysis of the startup current for the machine in Case III, based on the high-level detail signals.

Additional useful information can be obtained from Figure 14; there it can be seen that the component commented before which slightly distort the sideband evolution within approximation signal a_7, is contained here within the detail d_8. Therefore, the frequency evolution of this component is confined within the interval [11.7, 23.4] Hz, since this is the frequency band associated with d_8. This fact might help to find out the origin of that component, but it seems clear that it is not related with the breakage, the presence of which is confirmed through the aforementioned characteristic pattern in the high-level wavelet signals.

Fig. 14 also shows the partial penetration of the main frequency into the frequency band of detail d_7, since for f_s=6000 samples/s, the component of 50 Hz is too close to the upper limit of the frequency band of detail d_7 (46.9 Hz) . In this case this component is placed in the region where the frequency bands of d6 and d_7 overlaps (see Figure 9), masking completely the sideband evolution in d_7.

4.4. Case IV: 400 kW induction motor with clear asymmetry driving a coal mill fan

In this case, the sampling frequency was f_s= 4096 samples/s. Thus, according to (8) the number of

decomposition levels has to be set to n=6. The frequency band covered by the approximation signal a_6 is [0-32] Hz. Figure 15 shows the startup current of this machine, the approximation signal a_6 and, finally, a zoom of the central zone of a_6.

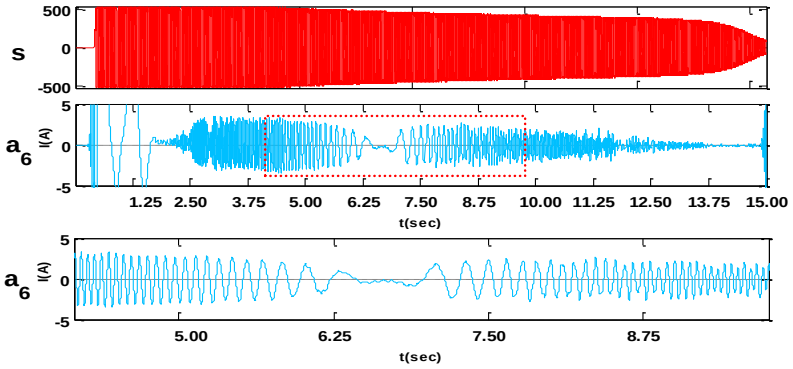

Figure 15. Tested current, approximation a_6, and its expanded representation for the startup of the machine in Case IV.

The characteristic evolution of the sideband component (with decreasing–increasing frequency) can be clearly recognized in the approximation signal a_6. The similarity with respect to the theoretical evolution of the left sideband shown in Figure 1 is evident. This leads to a consistent diagnostic of rotor asymmetry. Moreover, the value for the quantification parameter γ_{AP} is equal to 102.8 dB in this case, quite lower than for the machine of the Case II. This fact indicates the higher level of asymmetry for the current case.

5. CONCLUSIONS

The authors propose a methodology based on the extraction of the left sideband component from the stator startup current for the diagnosis of rotor bar breakages in cage motors. In the paper, two different signal processing tools (the Low Pass Filtering technique and the Discrete Wavelet Transform), enabling the easy extraction of this component, are explained and tested on industrial machines ranging from 1.1 to 450 kW. The results prove that this methodology is suitable for a wide scope of induction motor applications in which the startup length is not very short. This field involves applications of machines

with large powers or machines driving high inertias. This fact increases the interest of the proposed methodology since, for these applications, the probability of occurrence of bar breakages is high, as well as the cost of a fault not diagnosed in time or a wrong positive diagnostic. The tests have proved that, when this method is used under suitable conditions, even a single bar breakage can be diagnosed with a high reliability.

Moreover, parameters for quantifying the degree of severity of the fault have been defined for both approaches. In the case of the low pass filtering technique, a threshold value of 0.8 % for the quantification indicator can be considered as indicative of a significant level of asymmetry. In the case of the DWT, further tests have to be carried out for machines with different ranges of powers, in order to reach an accurate threshold for each power range. Nevertheless, according to the results a value lower than 102 dB could be considered as indicative of a significant asymmetry in machines larger than 200 kW.

It has to be remarked the robustness of both methods, since they enable the perfect extraction of the diagnosis signals, despite the possible problems when capturing the current signals (errors when selecting the scales amplitude for the waveform or errors in the time scale). This feature is very important in real applications dealing with large motors, in which is not always possible a second startup and in which the selection of the scales should be made approximately.

The comparison between both proposed techniques shows that the approach based on DWT presents some advantages, as for example, the simplicity of its application using commercial software packages and the possibility of simultaneous analysis of various frequency bands; this possibility enables improving the reliability of the diagnostic for some uncertain cases.

APPENDIX I: METHODOLOGY FOR CALCULATING THE EVOLUTION OF THE LEFT SIDEBAND HARMONIC DURING THE STARTUP.

The diagnosis approaches proposed in this paper are based on the identification of the characteristic shape of the left sideband component during the startup; Although the method for calculating the evolution of the left sideband harmonic during startup is explained with detail in [20], the authors deem interesting to include a summary of the main concepts on which the calculation process of this component is based.

- The method is based on the Deleroi approach [28], which states that the effects of broken bars can be analysed using the concept of "fault current". This is, the analysis of a machine with a broken rotor bar can be carried out considering the superposition of two configurations: the machine in healthy state, and the machine with a current source in the bar that breaks (fault current). The fault current is always equal to the current flowing through the same bar in the healthy machine but in the opposite direction, in such a way that the total current through the bar is null.

- The fault current creates a magnetic field in the airgap (fault field). The fault field is analyzed using the space vector theory, and an expression for the time evolution of the component of this field generating the left sideband (which is a sinusoidal-shaped rotating field) is deduced. This component, for a given time, depends on the RMS value of the rotor current and on the rotor speed.

- For a given machine and load conditions, the evolution of the rotor speed and rotor bar current is calculated during the startup using a numerical model of the induction motor. From the calculated currents and speed, the evolution of the space vectors of induction and yoke flux of the fault field component creating the left sideband are also calculated.

- Finally, the evolution of the left sideband component during the startup (see Figure 1) is calculated by using a conventional numerical model of the induction motor, but with the stator and rotor windings short-circuited (all the phase voltages are null) and with an imposed yoke flux wave in every

time that coincides with the yoke flux which generates the left sideband, calculated in the precedent step.

ACKNOWLEDGEMENTS

The research leading to these results has received funding from the European Community's Seventh Framework Programme FP7/2007-2013 under Grant Agreement n° 224233 (Research Project PRODI "Power plant Robustification based on fault Detection and Isolation algorithms"). The authors also thank 'Vicerrectorado de Investigación, Desarrollo e Innovación of Universidad Politécnica de Valencia' for financing a part of this research through the program 'Programa de Apoyo a la Investigación y Desarrollo (PAID-06-07).

REFERENCES

[1] W.T. Thomson, M. Fenger, "Current signature analysis to detect induction motor faults" *IEEE Industry Applications Magazine*, July/August 2001, pp. 26-34.

[2] M. H. Benbouzid, "A review of induction motors signature analysis as a medium for faults detection" *IEEE Transactions on Industrial Electronics*, Vol. 47, No. 5, October 2000.

[3] P. Jover Rodriguez, A. Belahcen, and A. Arkkio, "Signatures of Electrical Faults in Force Distribution and Vibration Pattern of Induction Motors", *IET Electric Power Applications,* Vol. 153, No. 4, pp. 523-529, 2006.

[4] M.F. Cabanas, F. Pedrayes, M.R. González, M.G. Melero, C.H. Rojas, G.A. Orcajo, J.M. Cano and F. Nuño "A new Electronic Instrument for the early detection of Broken Rotor Bars in Asynchronous Motors Working Under Arbitrary Load Conditions," *Proc. 5th IEEE International Symposium on Diagnostics, Electric Machines, Power Electronics and Drives SDEMPED 2005*, Vienna, Austria, pp. 29-34, September 7-9, 2005.

[5] J. Penman, M.N. Dey, A.J. Tait, W.E. Bryan, "Condition monitoring for electrical drives," *IEE Proceedings*, Vol. 133, pt. B, No. 3, pp. 142-148, May 1986.

[6] J.S. Hsu, "Monitoring of defects in induction motors through air-gap torque observation," *IEEE Transactions on Industry Applications*, Vol. 31, pp. 1016-1021, September/October 1995.

[7] S.F. Legowski, A.H.M. Sadrul Ula and A. M. Trzynadlowski, "Instantaneous Power as a Medium for the Signature Analysis of Induction Motors," *IEEE Transactions on Industry Applications*, Vol. 32, No. 4, pp. 904-909, July/August 1996.

[8] J. Milimonfared, H. Meshgin Kelk, S. Nandi, A. Der Minassians and H. A. Toliyat, "A novel approach for broken-rotor-bar detection in cage induction motors," *IEEE Transactions on Industry Applications*, vol. 35, no. 5, pp. 1000-1006, September/October 1999.

[9] J.F. Watson, N.C. Paterson and D.G. Dorrell, "The Use of Finite Element Methods to Improve Techniques for the Early Detection of Faults in 3-phase Induction Motors," *IEEE Transactions on Energy Conversion*, Vol.14, No. 3, pp. 655- 660, September 1999.

[10] A. Bellini, F. Filippetti, G. Franceschini, C. Tassoni and G.B. Kliman, "Quantitative evaluation of induction motor broken bars by means of electrical signature analysis", *IEEE Transactions on Industry Applications*, Vol. 37, No. 5, September/October 2001, pp 1248-1255

[11] R.R. Schoen, T.G. Habetler. "Evaluation and Implementation of a System to Eliminate Arbitrary Load Effects in Current-Based Monitoring of Induction Machines." *IEEE Transactions on Industry Application*s, Vol. 33, No. 6, November/December 1997, pp. 1571-1577

[12] R. Burnett and J.F. Watson, "The current analysis program – a software tool for rotor fault detection in three-phase induction motors," in *Proc. Inst. Elect. Eng. Elect. Machine drives*, 1995, pp.156-160.

[13] J.F. Watson and N.C. Paterson, "*Improved techniques for rotor fault detection in three-phase induction motors*," The 1998 IEEE Industry Applications Conference, 1998. Thirty-Third IAS Annual Meeting., vol.1, pp 271-277, 12-15 Oct 1998.

[14] J. Antonino-Daviu, M. Riera-Guasp, J. Roger-Folch and M.P. Molina, "Validation of a New Method for the Diagnosis of Rotor bar Failures via Wavelet Transformation in Industrial Induction Machines," *IEEE Transactions on Industrial Applications*, vol. 42, no. 4, July/August 2006.

[15] H. Douglas, P. Pillay, and A. Ziarani , "Broken rotor bar detection in induction machines with transient operating speeds," *IEEE Transactions on Energy Conversion*, vol. 20, no. 1, pp. 135-141, March 2005.

[16] Z. Zhang and Z. Ren, "A novel detection method of motor broken rotor bars based on wavelet ridge," *IEEE Transactions on Energy Conversion*, vol. 18, no. 3, pp. 417-423, September 2003.

[17] A.Stefani, F.Filippetti, A. Bellini, "Diagnosis of induction machines in time-varying conditions", *Diagnostics for Electric Machines, Power Electronics and Drives, 2007. SDEMPED 2007. IEEE International Symposium on,* 6-8 Sept. 2007 Page(s):126 – 131

[18] Bellini, A., "Quad Demodulation: A Time Domain Diagnostic Method for Induction Machines" *Industry Applications Conference, 2007. 42nd IAS Annual Meeting. Conference Record of the 2007 IEEE*, 23-27 Sept. 2007 Page(s):2249 – 2253.

[19] Kerszenbaum, I.; Landy, C.F, " The Existence of Large Inter-Bar Currents in Three Phase Squirrel Cage Motors with Rotor-Bar And/Or End-Ring Faults" *IEEE Transactions on Power Apparatus and Systems,* Volume PAS-103, Issue 7, July 1984 Page(s):1854 – 1862.

[20] M. Riera, J. Antonino-Daviu, J. Roger-Folch and M.P. Molina, "The Use of the Wavelet Approximation Signal as a Tool for the Diagnosis and Quantification of Rotor Bar Failures," *IEEE Transactions on Industry Applications,* Vol.44, pp 716-726, May/June 2008

[21] J. Antonino-Daviu, M. Riera-Guasp, J. Roger-Folch, F. Martínez-Giménez, A. Peris, "Application and Optimization of the Discrete Wavelet Transform for the Detection of Broken Rotor Bars in Induction Machines". *Applied and Computational Harmonic Analysis, Elsevier,* Vol. 21, No. 2 September 2006, pp. 268-279.

[22] G.B. Kliman, R.A. Koegl, J. Stein, R.D. Endicott, and M.W. Madden, "Noninvasive detection of broken rotor bars in operating induction motors," *IEEE Transactions on Energy Conversion*, vol. 3, no. 4, pp. 873-879, December 1988.

[23] N.M. Elkasabgy, A.R. Eastham, and G.E. Dawson, "Detection of broken rotor bars in the cage rotor on an induction machine" *IEEE Transactions on Industry Applications*, vol. 28, no. 1, pp. 165-171, January/February 1992.

[24] Rams W, Rusek J., "Practical Diagnosis of Induction Machines Operated in Power Plant Auxiliaries", *2005 IEEE St. Petersburg PowerTech Proceedings*, St. Petersburg 27-30.06.2005.

[25] C.S. Burrus, R.A. Gopinath and H. Guo, *Introduction to Wavelets and Wavelet Transforms a primer*, Prentice Hall, 1998

[26] C. K. Chui, *Wavelets: A Mathematical Tool for Signal Analysis*, SIAM, 1997.

[27] T. Tarasiuk, "Hybrid wavelet-Fourier Spectrum Analysis," *IEEE Transactions on Power Delivery*, Vol. 19, No. 3, July 2004, pp. 957-964.

[28] W. Deleroi "Squirrel cage motor with broken bar in the rotor –physical phenomena and their experimental assessment", *Proc. ICEM'82*. Budapest, Hungary, 1982, pp. 767-770